# Kinetic and Product Study of the Atmospheric Photooxidation of 1,4-Dioxane and Its Main Reaction Product Ethylene Glycol Diformate

**Tobias Maurer and Heinz Hass**

*FORD-Forschungszentrum Aachen, D-52068 Aachen, Germany*

**Ian Barnes* and Karl H. Becker**

*Bergische Universität GH Wuppertal/FB 9 - Physikalische Chemie, Gauss Strasse 20, D-42097 Wuppertal, Germany*

*Received: January 22, 1999; In Final Form: April 12, 1999*

A FTIR kinetic and product study of the OH-radical initiated oxidation of 1,4-dioxane (DOX) has been performed in a quartz-glass photoreactor in the laboratory under different conditions and also in the outdoor EUPHORE simulation chamber in Valencia, Spain. Using the relative kinetic technique, a rate coefficient of $k = (1.24 \pm 0.04) \times 10^{-11}$ cm$^3$ molecule$^{-1}$ s$^{-1}$ was determined for the reaction at 298 K in 1000 mbar of synthetic air, which is in good agreement with other published values. The major reaction product both in the presence and absence of NO was ethylene glycol diformate (EDF). This compound has been synthesized, and authentic samples have been used for calibration. Integrated band intensities have been calculated for the three strongest bands of EDF: $(4.99 \pm 0.06) \times 10^{-17}$ cm molecule$^{-1}$ for 1100−1225 cm$^{-1}$, $(3.90 \pm 0.05) \times 10^{-17}$ cm molecule$^{-1}$ for 1670−1820 cm$^{-1}$, $(9.34 \pm 0.11) \times 10^{-18}$ cm molecule$^{-1}$ for 2775−3075 cm$^{-1}$. In the laboratory reactor, yields for EDF of 87 ± 9 and 95 ± 10 mol % were obtained using the photolysis of MeONO/NO/air and $H_2O_2$/NO/air as the OH radical sources, respectively. Using only the photolysis of $H_2O_2$/air as the OH source resulted in a molar yield of 55 ± 6 mol % for EDF. In the outdoor EUPHORE simulation chamber a yield of 95 ± 10 mol % was obtained from irradiation of a DOX/$NO_x$/air mixture. The OH-radical- and Cl-atom-initiated oxidation of EDF has also been investigated. Rate coefficients of $k_{OH} = (4.72 \pm 0.31) \times 10^{-13}$ cm$^3$ molecule$^{-1}$ s$^{-1}$ and $k_{Cl} = (3.52 \pm 0.09) \times 10^{-12}$ cm$^3$ molecule$^{-1}$ s$^{-1}$ have been determined for the reaction of EDF with OH radicals and Cl atoms, respectively, at 298 K and 1000 mbar total pressure. The products determined in the Cl-initiated oxidation in the presence of $NO_x$ were formic acid anhydride (FAA), formic acid (FA), and carbon monoxide (CO) with yields of 173 ± 34 mol %, 45 ± 9 mol %, and 41 ± 8 mol %, respectively. Formation of a peroxy formyl nitrate was also observed. In the absence of $NO_x$ the yields of FAA, FA and CO were 144 ± 29 mol %, 39 ± 8 mol %, and 22 ± 4 mol %, respectively.

## Introduction

Branched and cyclic ethers are either currently in use or are under discussion as additives to fuels. The use of ethers in fuels[1] serves as a replacement for aromatic hydrocarbons, apart from enhancing the octane value they also help to reduce the carbon monoxide content of the automobile exhaust.[2] Ethers are also widely employed in industry as solvents. The cyclic ether 1,4-dioxane (DOX), for example, is mainly employed as a solvent for cellulose acetate, resins, oils, and waxes.[3]

The increased employment of DOX, and indeed any compound, as solvent or fuel additive inevitably results in increased emissions of these compounds to the atmosphere and raises the question of the atmospheric fate of the substances. The first major degradation step of most chemicals released into the troposphere is reaction with OH radicals. A detailed understanding of the kinetics and mechanisms of the reactions radicals with OH is, therefore, required in order to assess their potential atmospheric impact such as their contribution to the formation of ozone and other photooxidants or possible toxicity of the reaction products. DOX is a cyclic diether with symmetric structure and four equivalent $-CH_2-$ groups. There have been two previous determinations of the rate coefficient for the reaction of OH radicals with DOX (Dagout et al.[4] and Porter et al.[5]). Platz et al.[6] have examined the atmospheric chemistry of DOX and identified ethylene glycol diformate (EDF) as the only product with unit yield. However, the evidence for the identification and quantification was based on a comparison of the observed infrared product features with an infrared spectrum available in the literature.

We present here a kinetic and product study of the OH-radical initiated oxidation of DOX in which the major reaction product EDF has been identified and quantified using a synthesized sample of the pure compound. In addition, the variation of the yield of EDF with and without the presence of NO in the reaction system has been investigated. Further, first determinations have been made of the rate coefficients for the reaction of OH and Cl with EDF. Finally the products resulting from the Cl atom initiated oxidation with and without NO present have been identified.

## Experimental Section

The different experiment setups used for the investigations are described briefly below. Details can be found in the literature.[7−9] Most experiments were carried out in a 1080 l

* To whom correspondence should be addressed.

10.1021/jp990273k CCC: $18.00 
Published on Web 06/15/1999

quartz-glass room-temperature photoreactor equipped with a built-in White mirror system. Either the UV photolysis of hydrogen peroxide ($H_2O_2$) with 32 low-pressure mercury lamps (Philips TUV 40, $\lambda_{max} = 254$ nm) or the irradiation of methyl nitrite ($CH_3ONO$)/NO mixtures with 32 fluorescent lamps (Philips Tl 40W/05, $320 < \lambda < 450$ nm) was used for the production of OH radicals. Chlorine atoms were produced by the photolysis of molecular chlorine ($Cl_2$) with the fluorescent lamps. Concentration−time profiles of reactants and products were monitored by long path in situ FTIR spectroscopy. The FTIR spectrometer (Bruker IFS-88) was operated with a resolution of 1 $cm^{-1}$ using a path length of 484.7 m. All experiments were carried out at 1000 mbar total pressure in $O_2 + N_2$ at (298 ± 2) K. Measurements were performed with and without $NO_x$. During irradiation between 5 and 20 min, 10 spectra with 32/64/128 scans (0.5/1/2 min) were collected. Typical start concentrations employed for the product study were 1.2 ppm DOX, 0.5 ppm EDF, 1−2 ppm $CH_3ONO$, 10−20 ppm $H_2O_2$, 5−6 ppm $Cl_2$, and 0.5−10 ppm NO (1 ppm = $2.46 \times 10^{13}$ molecule $cm^{-3}$ at 1000 mbar and 298 K).

The rate coefficients for the reaction of OH with DOX and EDF were determined in the 1080 l photoreactor using the relative kinetic method.[10] In the case of EDF the Cl atom relative kinetic study was carried out in a 480 l Duran glass reactor in 1000 mbar of synthetic air at (298 ± 2) K. Detection of reactants was by in situ FTIR long path spectroscopy using a Nicolet 520 spectrometer and a path length of 51.6 m. The duration of one experiment was 40 min; over this period 20 spectra were collected with a resolution of 1 $cm^{-1}$ by coadding 83 scans per 2 min. Details can be found in the literature.[9]

In both the OH radical and Cl atom relative kinetic experiments, if there is no significant loss of the reactant (RA) or the reference (RF) compound by photolysis or wall loss, the observed decays can be described by

$$\mathrm{RA} + \mathrm{OH/Cl} \rightarrow \mathrm{Product}; \quad k_1$$

$$\mathrm{RF} + \mathrm{OH/Cl} \rightarrow \mathrm{product}; \quad k_2$$

and the kinetic data can be treated using eq 1

$$\ln \frac{[\mathrm{RA}]_{t=0}}{[\mathrm{RA}]_t} = \frac{k_{\mathrm{RA}}}{k_{\mathrm{RF}}} \ln \frac{[\mathrm{RF}]_{t=0}}{[\mathrm{RF}]_t} \qquad (1)$$

where $[RA]_{t=0}$ and $[RF]_{t=0}$ are the concentrations of the reactant and reference compound at time $t = 0$, respectively, and $[RA]_t$ and $[RF]_t$ are the concentrations at time $t$, and $k_{RA}$ and $k_{RF}$ are the corresponding rate coefficients for the reaction of reactant and reference compound with OH or Cl, respectively. Plots of $\ln([RA]_{t=0}/[RA]_t)$ against $\ln([RF]_{t=0}/[RF]_t)$ should yield a straight line with slope $k_{RA}/k_{RF}$ and zero intercept. The experiments were performed at 298 ± 2 K with propene ($k_{OH+propene} = (2.63 \pm 0.53) \times 10^{-11}$ $cm^3$ $molecule^{-1}$ $s^{-1}$)[11] as reference compound for the DOX + OH kinetic investigations and ethane ($k_{OH+ethane} = (2.50 \pm 0.10) \times 10^{-13}$ $cm^3$ $molecule^{-1}$ $s^{-1}$)[11] and ethyl chloride ($k_{Cl+ethyl\ chloride} = (8.7 \pm 1.0) \times 10^{-12}$ $cm^3$ $molecule^{-1}$ $s^{-1}$)[12] as reference compounds for the EDF + OH and EDF + Cl kinetic investigations, respectively. Typical start concentrations for the OH kinetic experiments were 1 ppm DOX, 0.5 ppm EDF, 4 ppm propene, 5 ppm ethane, and 25 ppm $H_2O_2$. For the kinetic experiments with Cl radicals 2−3 ppm EDF, 40 ppm ethyl chloride, and 40 ppm $Cl_2$ were used.

The infrared absorption cross sections of EDF were measured in a glass tube with a volume of 900 $cm^3$. The tube was evacuated, and vapor pressures of EDF between 0.7 and 0.25 mbar at (298 ± 2) K were established in the tube by injection of quantities of the compound. Spectra were recorded at a resolution of 1 $cm^{-1}$ over a path length of 46 cm with a Bruker IFS 88 FTIR spectrometer by coadding 128 interferograms over 2 min.

Three experiments on the OH-radical initiated oxidation of DOX were carried out in the outdoor EUPHORE[8] simulation chamber in Valencia, Spain. The chamber consists of a half-spherical 200 $m^3$ Teflon bag with a transmission of more than 80% of the sunlight between 280 and 640 nm and a cooling system under the chamber floor panels to compensate the heating of chamber by solar radiation. The photooxidation was initiated in the chamber by irradiation of a mixture of DOX and nitrogen oxide (NO) or nitrogen dioxide ($NO_2$) in 1000 mbar of dry air with natural sunlight. The concentration−time profiles of reactants and products were monitored by in situ FTIR-spectroscopy with a Nicolet Magna 550 spectrometer using a resolution of 1 $cm^{-1}$ and a path length of 326 m. Each spectrum consisted of 515 interferograms co-added over a time period of 15 min. Typical start concentrations were 400−770 ppb DOX and 50 ppb NO or 45 ppb $NO_2$, and the mixtures were irradiated for approximately 6 h.

**Chemicals and Gases.** 1,4-Dioxane (99+% GC) was purchased from Aldrich and hydrogen peroxide (85.0%) from Peroxid Chemie. Ethane 3.5, propene 3.5, $Cl_2$ 2.8, NO (≤ 99.95%), $NO_2$ 3.5, ethyl chloride 2.0, and synthetic air (99.995%) were supplied by Messer Griesheim with the stated purities.

Methyl nitrite was synthesized as described in the literature[13] by adding sulfuric acid dropwise to an ice cooled mixture of methanol and sodium nitrite and collection in a cold trap at −76 °C. The reference spectra of formic acid anhydride, formic acid and carbon monoxide were taken from an available calibrated infrared spectrum data bank collected by this group.

EDF was synthesized in a manner similar to a method described in the literature for *t*-amyl formate.[14] Briefly, mixed anhydride (formic and acetic acid) was slowly added to ethylene glycol and stirred at room temperature for 24 h. The mixture was than neutralized with a saturated solution of sodium bicarbonate, washed with water, and extracted with dimethyl ether. Separation of the product was performed by distillation under reduced pressure. The purity of the compound was determined by GC/ NMR with >98%.

**Spectroscopic Data.** (IR (vapor) C═O 1754 $cm^{-1}$, C−H 2942 $cm^{-1}$, C−O 1162 $cm^{-1}$; $^1H$ NMR ($CDCl_3$, 400 MHz) $\delta = 7.97$ ppm (s, 2H, −OC(O)-H), $\delta = 4.29$ ppm (s, 4H, $-CH_2-$); $^{13}C$ NMR ($CDCl_3$, 400 MHz) $\delta = 160.7$ ppm (−OC(O)H), $\delta = 61.6$ ppm ($-CH_2-$).

## Results

**Rate Coefficients for the Reaction of 1,4-Dioxane (DOX) with OH Radicals and Ethylene Glycol Diformate (EDF) with OH Radicals and Cl Atoms.** Over the time period of all the experiments both adsorption on the wall and photolysis of the compounds were negligible. Figure 1, parts A and B, shows examples of the data from the kinetic experiments plotted according to eq 1 for the reaction of OH with DOX and Cl with EDF, respectively. From slopes of these plots the following rate coefficients have been derived were the quoted errors, which do not include possible errors in the reference rate coefficient, represent the uncertainty at the 95% confidence level:

$$k_{\mathrm{OH-DOX}} = (1.24 \pm 0.04) \times 10^{-11}\,\mathrm{cm^3\,molecule^{-1}\,s^{-1}}$$

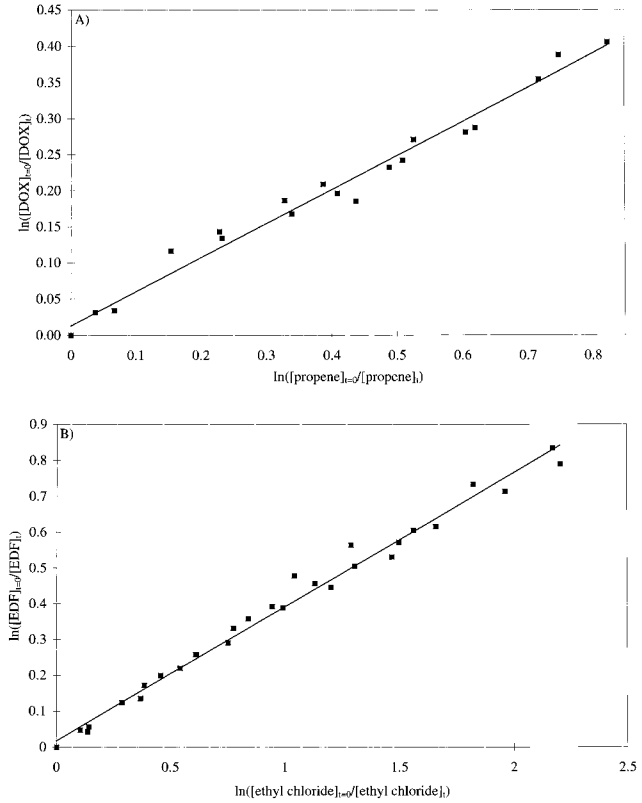


**Figure 1.** Kinetic data plotted according to eq 1 for reaction of (A) OH radicals with 1,4-dioxane (DOX) and (B) Cl atoms with ethylene glycol diformate (EDF).

$$k_{\mathrm{OH-EDF}} = (4.72 \pm 0.31) \times 10^{-13}\ \mathrm{cm^3\,molecule^{-1}\,s^{-1}}$$

$$k_{\mathrm{Cl-EDF}} = (3.52 \pm 0.09) \times 10^{-12}\ \mathrm{cm^3\,molecule^{-1}\,s^{-1}}$$

Infrared integrated band intensity (IBI) of ethylene glycol diformate (EDF). Figure 2 shows the infrared spectrum of EDF (spectrum C) recorded with a resolution of 1 $cm^{-1}$ in the region of 700 to 2000 $cm^{-1}$. The spectrum contains three main absorption bands, one in the region of the C−H stretching vibration between 2875 and 3075 $cm^{-1}$ (not shown in Figure 2), one in the region of the C═O stretching vibration between 1670 and 1820 $cm^{-1}$, and one in the region of the C−O stretching vibration between 1100 and 1225 $cm^{-1}$. For these three bands the following integrated band intensities (IBI) have been calculated where the estimated errors represent the uncertainty at the 95% confidence level:

$$\mathrm{IBI}\ (2775-3075\ \mathrm{cm^{-1}}) = (9.34 \pm 0.11) \times 10^{-18}\ \mathrm{cm\,molecule^{-1}}$$

$$\mathrm{IBI}\ (1670-1820\ \mathrm{cm^{-1}}) = (3.90 \pm 0.05) \times 10^{-17}\ \mathrm{cm\,molecule^{-1}}$$

$$\mathrm{IBI}\ (1100-1225\ \mathrm{cm^{-1}}) = (4.99 \pm 0.06) \times 10^{-17}\ \mathrm{cm\,molecule^{-1}}$$

**Products from the OH-Radical Initiated Oxidation of 1,4-Dioxane(DOX).** Figure 2 shows infrared spectra obtained from the experimental system with $NO_x$. Part A shows a spectrum recorded before radiation, B is a difference of a spectrum recorded after 10 min irradiation minus spectrum A, C is the EDF reference spectrum, and D is the residual product spectrum

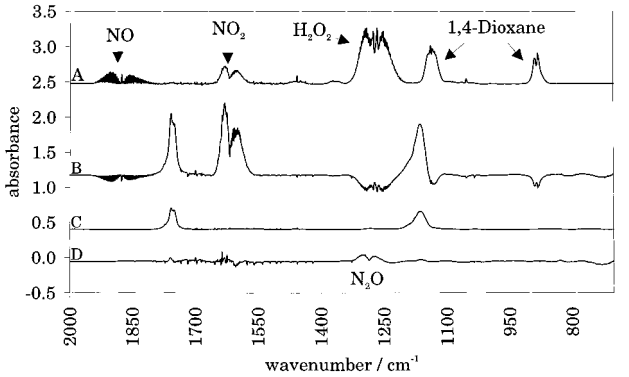


**Figure 2.** Infrared spectra recorded for a $H_2O_2/NO_x$/DOX photolysis system in the wavenumber region 2000−700 $cm^{-1}$. Spectrum A was recorded before irradiation, B is a difference spectrum derived from a spectrum recorded after 10 min irradiation minus spectrum A, C is a reference spectrum of EDF, and D is the residual spectrum obtained after 10 min irradiation and subtraction of DOX and all identified products. The $N_2O$ is introduced into the chamber as impurity with NO.

**TABLE 1: Molar Yields of Ethylene Glycol Diformate (EDF) Obtained from Experiments on the OH-Radical-Initiated Oxidation of 1,4-Dioxane (DOX)**

| part | reactor | condition | OH-source | light source | EDF yield[a] (mol%) |
|---|---|---|---|---|---|
| A | 1080 L reactor | without $NO_x$ | $H_2O_2$ | UV | 55 ± 6 |
| B | 1080 L reactor | with $NO_x$ | $H_2O_2$ | UV | 95 ± 10 |
| C | 1080 L reactor | with $NO_x$ | $CH_3ONO$ | vis | 87 ± 9 |
| D | 200 $m^3$ smog chamber | with $NO_x$ | $NO_x$/RH | sunlight | 95 ± 10 |

[a] The errors are estimated for a relative uncertainty of 10%.

obtained after subtraction of all identified compounds. The $N_2O$ in spectrum D is introduced into the chamber as impurity with NO. In contrast to the residual spectrum of the $NO_x$-containing system, significant absorptions in the area of the C═O stretching vibration between 1750 and 1650 $cm^{-1}$ and in the area of the C−O stretching vibration between 1200 and 1000 $cm^{-1}$ remain in the $NO_x$-free system (not shown).

From the analysis of the infrared data with the calibrated EDF spectrum the main product of the OH-initiated oxidation of DOX has been positively identified as EDF in all of the systems investigated. The EDF molar yield for the different experimental systems has been obtained from the slopes of plots of the concentration of EDF formed against reacted DOX. Examples of such plots for a $NO_x$-containing (part A)) and a $NO_x$-free system (part B)) are shown in Figure 3. The molar yields of EDF obtained for the different experimental systems are summarized in Table 1. The EDF yields have not been corrected for secondary reaction with OH radicals since this reaction is slow and over the time scale of the experiments the correction is negligibly small.

**Products from the Cl-atom-initiated oxidation of ethylene glycol diformate (EDF).** Because of the very slow reaction of EDF with OH radicals the Cl-atom initiated oxidation was used to study the products with and without $NO_x$ in the reaction system. The oxidation processes with OH radicals and Cl atoms are very similar and only minor differences in site selectivity is expected.

Figure 4 shows infrared spectra obtained from the experimental system with $NO_x$. Shown in part A is a spectrum recorded before irradiation, B is a difference spectrum derived from a spectrum recorded after 10 min irradiation minus spectrum A, C is a calibrated reference spectrum of formic acid anhydride (FAA),[15] and D is the residual spectrum obtained after

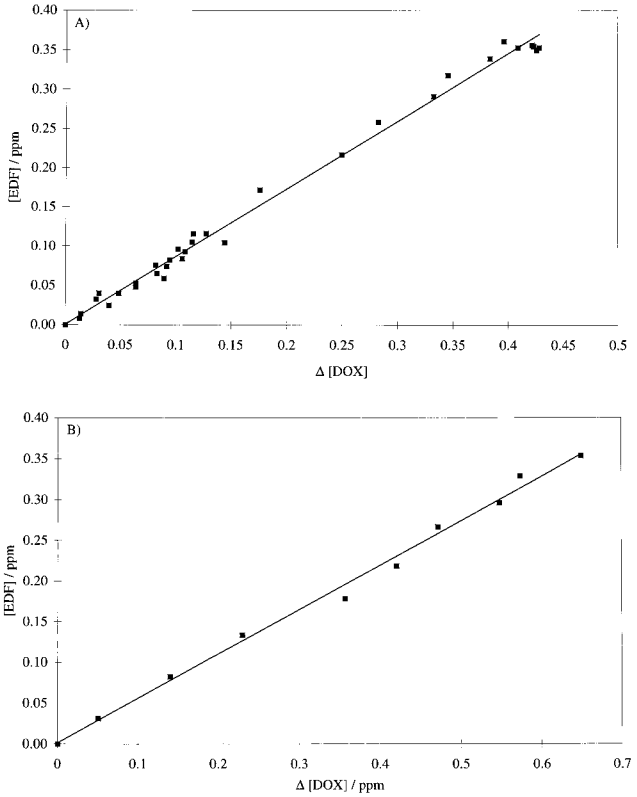


**Figure 3.** Example of a plot of the measured EDF concentration versus the amount of DOX consumed for the OH-radical-initiated oxidation using (A) the photolysis of $CH_3ONO/NO/air$ as the OH-radical source and (B) the photolysis of $H_2O_2$ as the radical source.

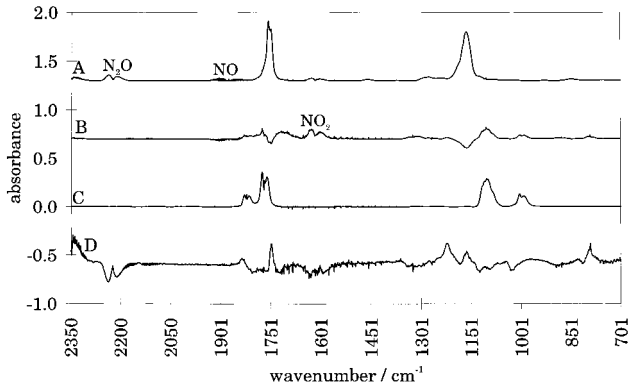


**Figure 4.** Infrared spectra obtained from a $Cl_2/NO/$ethylene glycol diformate (EDF) photolysis system in the wavenumber region 2350−700 $cm^{-1}$. Spectrum A was recorded before irradiation, B is a difference spectrum derived from a spectrum recorded after 10 min irradiation minus spectrum A, C is a calibrated reference spectrum of formic acid anhydride (FAA), and D is the residual spectrum obtained after 10 min irradiation and subtraction of EDF and all identified products multiplied by a factor of 10.

10 min irradiation and subtraction of EDF. All of the absorption values of the identified products are multiplied by a factor of 10 in order to better highlight the residual absorptions.

In reaction systems with or without $NO_x$, three products were identified, formic acid anhydride (FAA), formic acid (FA), and carbon monoxide (CO). Molar yields for the products have been obtained from plots of the measured concentrations as a function of EDF reacted as illustrated by the exemplary plots in Figure 5 for a $Cl_2/NO/EDF$ photolysis experiment. The measured molar yields are listed in Table 2.

In the residual product spectrum of the $NO_x$-free system only weak residual absorptions remain after subtraction of the

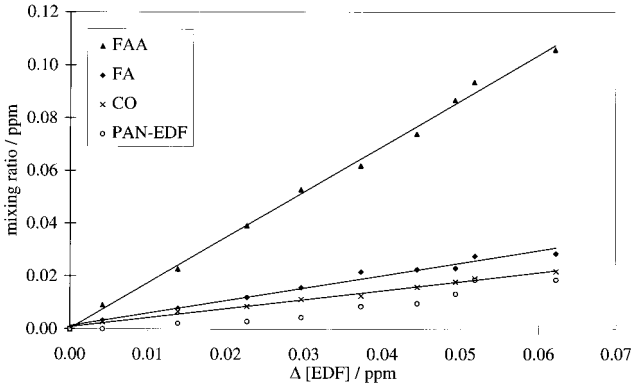


**Figure 5.** Plots of the measured concentrations of formic acid anhydride (FAA), formic acid (FA), and CO as a function of the amount of ethylene glycol diformate (EDF) consumed. The data are from a $Cl_2/NO/EDF$ photolysis experiment. The plot of the data for the peroxy formyl nitrate (PAN-EDF) shows curvature, the increase in slope with the amount of consumed EDF is due to changes in the $NO/NO_2$ ratio as described in the text.

**TABLE 2: Molar Yields of Products Observed in the Cl-Atom-Initiated Oxidation of Ethylene Glycol Diformate (EDF) in Presence and Absence of $NO_x$**

| product of EDF oxidation | molar yields %[a] [Cl, synthetic air] | molar yields %[a] [Cl/NO, synthetic air] |
|---|---|---|
| formic acid anhydride (FAA) | 144 ± 29 | 173 ± 34 |
| formic acid (FA) | 39 ± 8 | 45 ± 9 |
| carbon monoxide (CO) | 22 ± 4 | 41 ± 8 |

[a] Errors are the total overall estimated uncertainty of 20%.

identified products in the region at 1150 $cm^{-1}$; however, in the residual product spectrum from the system with $NO_x$ (see Figure 4 spectrum D) distinctive spectral features remain with bands at 1835, 1746, 1306, 1223, and 793 $cm^{-1}$. These absorptions are very similar to the characteristic absorptions of peroxy acetyl nitrate (PAN) and are consequently assigned to a peroxy formyl nitrate (PAN-EDF). The formation of this compound is dependent on the $NO/NO_2$ ratio in the experimental system and consequently the yield at the beginning of the experiment with high $NO/NO_2$ ratio is low and increases gradually during the course of the experiment as the $NO/NO_2$ ratio decreases. A rough estimate has been made of the concentration of the peroxynitrate using the value of $1.09 \times 10^{-3}$ $ppm^{-1}$ $m^{-1}$ for the absorption cross section of peroxy acetyl nitrate at 1835 $cm^{-1}$ available in the literature[16]; its yield is found to vary between approximately 8 and 30 mol % during the progression of an experiment.

## Discussion

**Kinetic Experiments.** The measured rate coefficient for the reaction of DOX with OH is in reasonable agreement with the values reported in the literature. The value reported by Porter et al.[5] ($k = 1.26 \cdot 10^{-11}$ $cm^3$ $molecule^{-1}$ $s^{-1}$) using an absolute technique agrees best with that measured in the present work. It is somewhat higher than the values measured by Dagaut et al.[4] ($k = 1.09 \cdot 10^{-11}$ $cm^3$ $molecule^{-1}$ $s^{-1}$) and Porter et al.[5] ($k = 9.7 \cdot 10^{-12}$ $cm^3$ $molecule^{-1}$ $s^{-1}$) using absolute and relative techniques, respectively.

The measured rate coefficient for the reaction of OH with DOX is lower than the value of $k = 3.9 \cdot 10^{-11}$ $cm^3$ $molecule^{-1}$ $s^{-1}$ calculated using the structure activity relationship (SAR) technique. The rate can be compared with that of the open chain diether dimethoxy ethane (DMEt), $CH_3OCH_2CH_2OCH_3$, which contains one $-OCH_2CH_2O-$ unit. Rate coefficients of (3.3 ±

$0.2) \times 10^{-11}$ cm$^3$ molecule$^{-1}$ s$^{-1}$ [5] and $(2.7 \pm 0.5) \times 10^{-11}$ cm$^3$ molecule$^{-1}$ s$^{-1}$ [17] have been reported in the literature for the reaction of DMEt with OH-radicals. The value is slightly more than a factor of 2 higher than that measured for DOX which contains 2 $-CH_2CH_2-$ units joined in a cyclic fashion by 2 ether linkages. Porter et al.[5] have postulated that this apparent discrepancy can be explained by the formation of six-membered cyclic transition state in the case of the reaction of OH with the linear ether dimethoxy ethane which is not possible in the case of the cyclic ether DOX.

To our knowledge this represents the first determination of the rate coefficients for the reaction of OH radicals and Cl atoms with EDF. Because of the lack of data for the formate group, it is difficult to reliably estimate a rate coefficient for the reaction of OH with EDF using the SAR method. A survey of the kinetic data for other formates in the literature,[18,19] shows that the presence of a formate group greatly reduces the reactivity of a compound. For example, if DMEt[5] is compared with methoxy ethyl formate,[17] $CH_3OCH_2CH_2OCHO$, replacing one of the two $CH_3O$-groups by a formate group decreases the OH rate coefficient by a factor of approximately 6.5 from $(3.3 \pm 0.2) \times 10^{-11}$ cm$^3$ molecule$^{-1}$ s$^{-1}$ to $(5.10 \pm 1.03) \times 10^{-12}$ cm$^3$ molecule$^{-1}$ s$^{-1}$. If such effects are additive one would predict a value of approximately $7.9 \times 10^{-13}$ cm$^3$ molecule$^{-1}$ s$^{-1}$ for the reaction of OH with EDF which considering the crude approximation is in fair agreement with the actual measured value of $(4.72 \pm 0.31) \times 10^{-13}$ cm$^3$ molecule$^{-1}$ s$^{-1}$. The rate coefficient of $(3.52 \pm 0.09) \times 10^{-12}$ cm$^3$ molecule$^{-1}$ s$^{-1}$ is intermediate between the values of $(1.83 \pm 0.21) \times 10^{-12}$ and $(13.4 \pm 0.15) \cdot 10^{-12}$ cm$^3$ molecule$^{-1}$ s$^{-1}$ reported for the reaction of Cl with the simple formates methyl and ethyl formate, respectively.[20]

For both the OH-radical and Cl-atom, H-atom abstraction from the formate group is known to be very slow. Therefore, in the OH- and Cl-initiated oxidation of DOX, H-atom abstraction from the $-OCH_2CH_2O-$ moiety is expected to dominate over abstraction from the formate group. For example, the rate coefficient for the reaction of Cl-radicals with formic acid is $(2.00 \pm 0.25) \times 10^{-13}$ cm$^3$ molecule$^{-1}$ s$^{-1}$ [21] and is thought to proceed mainly by H abstraction from the $H-CO-$ group. Using this value suggests that for the reaction of Cl with EDF approximately 11% should proceed via H atom abstraction from the formate group and the remainder from the $-OCH_2CH_2O-$ moiety.

**Products Studies on 1,4-Dioxane (DOX).** The product studies show quite conclusively that, in the presence of $NO_x$, the OH-radical oxidation of DOX leads to the formation of EDF in near 100% yield. The result confirms the earlier assignment of Platz et al.[6]. However, the results obtained in the absence of $NO_x$ differ significantly from those of Platz et al. In the present study a yield of 55 mol % is found for EDF without $NO_x$; whereas Platz et al. found only 10 mol % less EDF in their $NO_x$-free system compared to their $NO_x$-containing system.

The reaction of OH with DOX can only proceed via an H-atom abstraction mechanism to form EDF and because of its symmetric cyclic structure all the $-CH_2-$ groups are equivalent. Figure 6 shows the reactions in the oxidation of DOX, with and without $NO_x$ in the system, which lead to the formation of EDF and other possible products. The reactions dominating under most atmospheric conditions are highlighted by the arrows in bold type. Irrespective of whether $NO_x$ is present or not the first step is abstraction of a ring H atom followed by addition of $O_2$ to form a cyclic alkylperoxy radical (**I**). With NO this is transformed to a cyclic alkoxy radical (**II**), which reacts further by cleavage of the C−C bond to form an open chain alkoxy radical with one formate group (**III**). In the presence of NO reaction of the cyclic alkoxy radical (**II**) with $O_2$ to form a lactone (**VI**) ether and $HO_2$ appears to be negligible. The open chain alkoxy radical (**III**) reacts with $O_2$ to form a peroxy radical (**IV**), which further reacts with NO to form the alkoxy radical (**V**). EDF is then formed via reaction of this alkoxy radical with $O_2$. Isomerization reactions of radical (**V**) appear to be unimportant. This is supported by the 100% carbon balance and the lack of observation of FAA, FA, and HCHO which are expected isomerization products.

The oxidation mechanism of the DOX in a $NO_x$-free system is more complicated because of the self-and cross peroxy radical reactions, which can occur as shown in Figure 6. Reaction steps which can affect the EDF yield are the self-reaction of the cyclic peroxy radicals (**I**) giving the lactone (**VI**) and alcohol (**VII**) or reaction of the peroxy radicals (**I**) with $HO_2$ to form a hydroperoxide (**VIII**). The self-reaction of the open chain peroxy radical (**IV**) to form an alcohol (**IX**) or with $HO_2$ to form a hydroperoxide (**X**) can also affect the EDF yield.

As can be seen from Table 1, in the absence of $NO_x$ the yield of EDF in the oxidation of DOX is only 55 mol %. Varying the $O_2$ partial pressure between 0 and 600 mbar at a total pressure of 1000 mbar ($N_2 + O_2$) did not affect the EDF yield. This observation is consistent with the results of Platz et al.[6] who also found no dependence of the EDF formation yield on the $O_2$ concentration. The missing 45 mol % products are likely to consist of ether lactone (**VI**), an alcohol (**VII** and **IX**), and a hydroperoxide (**VIII** and **X**). In the residual product spectrum of a $NO_x$ free system the absorption observed at 1760 cm$^{-1}$ is typical for six-membered lactones and that at 3460 cm$^{-1}$ probably belongs to a hydroperoxide. Absorptions in the region of 3500 to 3700 cm$^{-1}$, which are typical for alcohols, were not observed.

The reason for the considerably lower yield of EDF in this study measured in the absence of $NO_x$ compared to that of Platz et al.[6] is not clear. Platz et al. used high concentrations of $Cl_2$ in their study and probably had high steady-state concentrations of Cl-atoms. The reactions of Cl-atoms with peroxy radicals are fast; it may be that in the system of Platz et al. peroxy−peroxy reactions were suppressed by efficient conversion of the peroxy radicals to alkoxy radicals via reaction with Cl atoms.

**Products Studies on Ethylene Glycol Diformate.** The major product observed in the Cl-atom-initiated oxidation of EDF is FAA with yields of 86 ± 17%C in the presence of $NO_x$ and 72 ± 15%C without $NO_x$ in the system. The other products observed are FA and CO. The carbon balances were 108 ± 21% and 87 ± 18% with and without $NO_x$, respectively, showing that all the major products have been identified. The yields of CO and FA were approximately the same in the system with $NO_x$; however, in the $NO_x$-free system the CO yield is approximately half the FA yield. The observation of a PAN-type product in the presence of $NO_x$ shows that H-abstraction also occurs at the terminal formate H-atoms. Although no evidence could be found for the presence of other products in the residual spectra after subtraction of the identified products the carbon balance in the absence of $NO_x$ suggests that small amounts of other products may be formed.

With the exception of the PAN-type compound plots of the concentration of all the observed products against the amount of EDF reacted are linear as it is shown by the exemplary plots in Figure 5 for the $NO_x$-containing system. The linearity of the plots supports that the products are all formed directly and not in secondary reactions. The reason for the nonlinear behavior

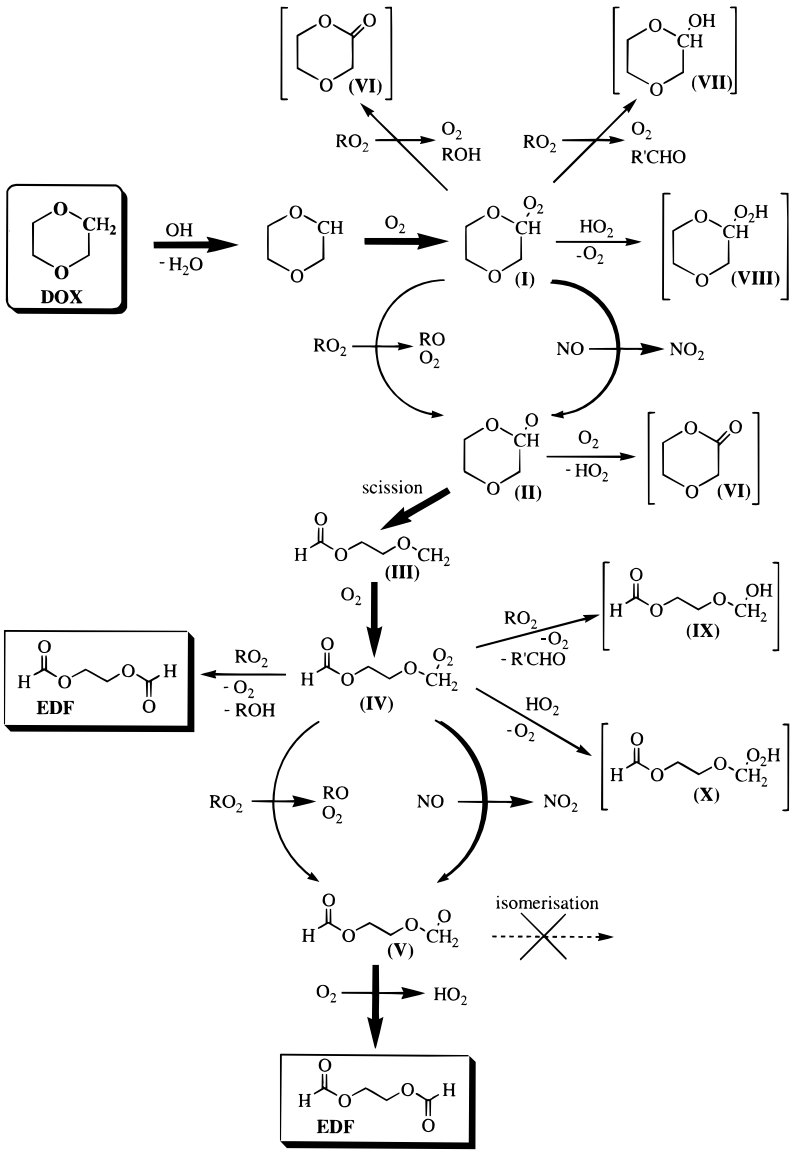


**Figure 6.** Mechanism for the OH-radical-initiated oxidation of 1,4-dioxane (DOX) depicting possible reaction channels both with and without the presence of $NO_x$. The reactions dominating under most atmospheric conditions showing arrows with bold type.

of the PAN-type compound is due to the variation of the NO/$NO_2$ ratio with time as discussed earlier.

As for DOX, both the OH-radical- and Cl-atom-initiated oxidation of EDF will proceed by H-atom abstraction. However, in contrast to DOX, there are two different positions for radical attack i.e., H-atom abstraction from either the H−C(O)−O− or the O−$CH_2CH_2$O− entities leading to the corresponding alkyl radicals.

From the discussion in the kinetic section it is expected that in the $Cl_2$ system used for the product analysis approximately 89% of the Cl-atom attack will be at the methylene groups in the center of the molecule (see Figure 7). Attack at the methylene group will lead to formation of the alkoxy radical HC(O)OCH(O•)$CH_2$OC(O)H (XI) which can decompose giving two molecules of FAA (**XII**/**XIIb**) as shown in Figure 7. No indication was observed for the formation of a mixed anhydride (**XIII**) by reaction of the alkoxy radical (**XI**) with $O_2$. This supports that the alkoxy radical undergoes C−C bond scission rather than reaction with $O_2$ as has been observed for similar peroxy radicals formed from other ethers, e.g., DOX. Decomposition of FAA in the liquid phase is known to produce FA;[22] however, the short time scale and a stability test performed in the reactor rules out this route as the source of this product.

Tuazon et al.[23] have recently reported that alkoxy radicals of structure RC(O)OCH(O•)R can undergo a rapid rearrangement and decomposition to RC(O)OH and RC(•)O via a five-membered ring transition state. The authors observed the so-called "α-ester rearrangement" for several acetates. This type of rearrangement is possible with the HC(O)OCH(O•)$CH_2$-OC(O)H (**XI**) radical formed from the oxidation of EDF. The α-ester rearrangement for this radical is shown in Figure 7. The rearrangement would result in formation of FA (**XIV**) and is obviously a possible source of the acid in this study. The α-ester rearrangement of the HC(O)OCH(O•)$CH_2$OC(O)H radical apart from forming FA will give the C(O•)$CH_2$OC(O)H radical (**XV**). The fate of this radical is expected to be addition of $O_2$ and eventual cleavage of $CO_2$ with formation of the (•)$CH_2$OC(O)H radical (**XVI**). This radical is also formed in the C−C bond scission of radical (**XI**). The further reactions of (•)$CH_2$OC-(O)H will give (•O)$CH_2$OC(O)H (**XVII**). The (•O)$CH_2$OC(O)H radical can either react with $O_2$ to produce FAA (**XIIb**) or undergo an α-ester rearrangement to form FA (**XIVb**) and HCO. Further reaction of HCO with $O_2$ will give CO.

The approximately equal yields of FA and CO and also the somewhat higher yield of FAA in the reaction system with NO suggests that in the NO-system the major reaction of the HC-

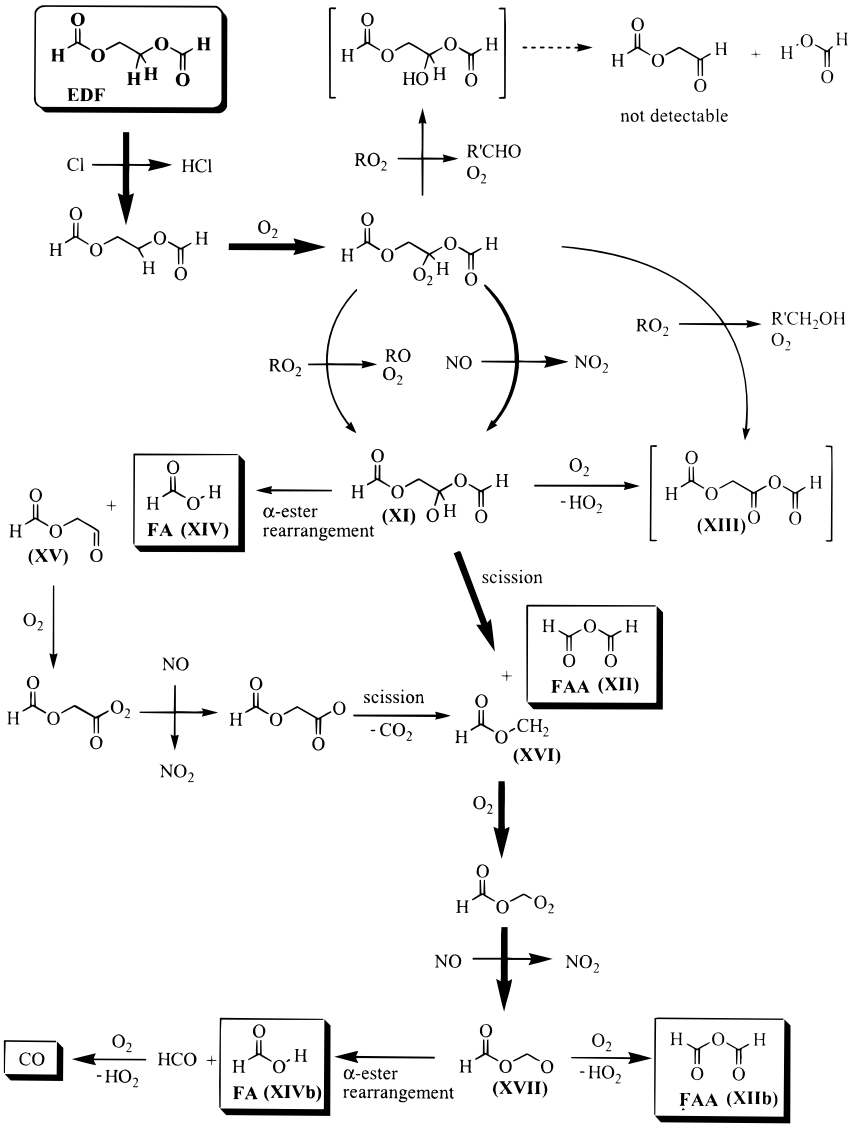


**Figure 7.** Mechanism for the Cl-atom initiated oxidation of ethylene glycol diformate (EDF) depicting reaction channels with Cl attack at the methylene group. To maintain clarity the reaction channels involving $RO_2$ are only shown in the initial steps. The reactions dominating under most atmospheric conditions showing arrows with bold type.

(O)OCH(O•)$CH_2$OC(O)H (**XI**) radical will be the C−C bond cleavage and that the α-ester rearrangement is negligible. If the α-ester rearrangement channel was operative to any degree, a disproportionation between the yields of FA and CO would occur, i.e., higher yields of FA compared to those of CO. This is exactly what is observed in the $NO_x$-free experiments where the yield of CO is approximately a factor of 2 lower than the FA yield. A possible explanation of this effect may be the formation of a "hot alkoxy radical" in the NO-containing system. The "hot alkoxy radical" effect has recently been postulated to explain differences between the behavior of several alkoxy radicals in the presence and absence of NO.[24] This effect causes a significant fraction of the available energy to be deposited into the internal modes of the oxy radical product, which results in an enhanced tendency for the radical to undergo unimolecular decomposition. Thus, in the present case, in the presence of NO, formation of a "hot alkoxy radical" favors C−C bond fission over an α-ester rearrangement. While, in the absence of NO the peroxy-peroxy reactions forming the oxy radical are not so exothermic and consequently the oxy radical will be less excited and α-ester rearrangement can occur to some extent. On the basis of the yield of CO and FA as coproduct, the results

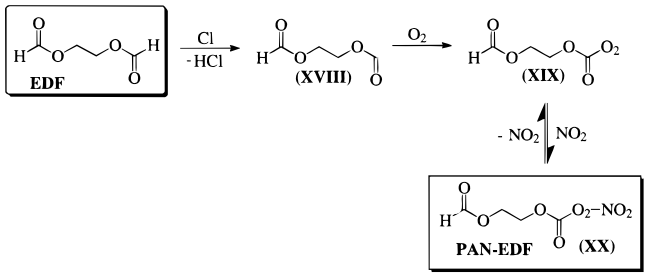


**Figure 8.** Mechanism for the formation of the PAN-EDF in the reaction of ethylene glycol diformate (EDF) with Cl-atoms.

are in line with radical (**XI**) in Figure 7 undergoing approximately 83% C−C scission and 17% α-ester rearrangement in the absence of $NO_x$. Radical (**XVII**) cannot undergo C−C bond scission. From a comparison of the FA to CO yields in the NO-containing system it is estimated that the $O_2$ reaction and α-ester rearrangement account for approximately 63 and 37%, respectively, of the fate of this radical.

Abstraction of the H atom at the formate group forms an alkoxy-radical (**XVIII**) which adds $O_2$ to form the peroxyradical (**XIX**) as shown in Figure 8. In the presence of $NO_x$ addition

of $NO_2$ leads to the peroxy formyl nitrate (PAN-EDF) (**XX**). In the absence of $NO_x$ reactions of the formylperoxy radicals (**XIX**) and formyloxy will occur. The products of these reaction are not known but will probably produce $HCO-O-CH_2CH_2-O(^{\bullet})$ radicals and eventually HC(O)-O−$CH_2$CH(O). Although a PAN-type compound is formed in the Cl-atom initiated oxidation it is not expected that PAN formation will be important in the OH-radical initiated oxidation, since OH should be more site selective and attack at the methylene group is expected to dominate.

## Conclusions

The atmospheric oxidation of 1,4-dioxane (DOX) and ethylene glycol diformate (EDF) has been studied under different conditions. It has been confirmed, using an authentic sample, that EDF is the only product of the OH initiated oxidation of DOX in the presence of NO with a molar yield of about 100% independent of OH source. In the absence of $NO_x$ the yield of EDF is only 55% indicating the formation of other nonidentified products such as cyclic esters, alcohols or hydroperoxides. The rate coefficient determined for the reaction of OH with DOX of $k = (1.24 \pm 0.04) \times 10^{-11}$ cm$^3$ molecule$^{-1}$ s$^{-1}$ is in good agreement with other literature values.

Rate coefficients of $(4.72 \pm 0.31) \times 10^{-13}$ and $(3.52 \pm 0.09) \times 10^{-12}$ cm$^3$ molecule$^{-1}$ s$^{-1}$ have been determined for the reaction of OH-radicals and Cl-atoms with EDF, respectively.

Using an annual average global tropospheric OH concentration of $1 \times 10^6$ molecules cm$^{-3}$ [25] the maximum lifetime of DOX and EDF will be 22.4 h and 24 days, respectively. The lifetime of EDF with respect to reaction with OH will enable it to be transported to remote areas. However, because of the good solubility of EDF in water, wet precipation or rain out will be an important loss process which will considerably shorten its atmospheric lifetime in humid or wet climatic regions.

The products of the Cl-atom initiated EDF oxidation, in order of importance, are formic acid anhydride (FAA), formic acid (FA), and carbon monoxide (CO). The yields of all compounds were highest in a system containing NO. A mechanism has been proposed to explain the formation of the products. The formation of FA and CO includes an α-ester rearrangement recently invoked to explain the acid formation in the oxidation of acetates.

The oxidation of DOX and cyclic diethers in general will lead to formation of alkyl diformates. The major atmospheric loss processes for these alkyl diformates will be gas phase reaction with OH radicals and wet precipitation. Both of these processes will result in acid formation, mainly formic acid, and the widespread use of ethers could, therefore, lead on the long term to an increase in the atmospheric acid burden.

**Acknowledgment.** Financial support of the work by the European Commission and the "Bundesministierum für Bildung und Forschung" (BMBF) is gratefully acknowledged. The authors acknowledge the help of the CEAM employees in using EUPHORE and financial support by the Generalidad Valenciana and Fundación BANCAIXA.

## References and Notes

(1) Hälsig, C.-P.; Gregory, R.; Peacock, T. *Special Publication−Royal Society of Chemistry Chemicals in the Oil Industry: Developments and Applications* **1991**, *97*, 311.

(2) Dolislager, L. J.; J. *Air Waste Manag. Assoc.* **1997**, *47*, 775.

(3) *Rev. of Environ. Contam. Toxicol.* **1988**, *106*, 113 (Section I), based on USEPA, 1987.

(4) Dagaut, P.; Wallington, T. J.; Liu, R.; Kurylo, M. J. *J. Phys. Chem.* **1990**, *94*, 1881.

(5) Porter, E.; Wenger, J.; Treacy, J.; Sidebottom, H.; Mellouki, A.; Téton, S.; Le Bras, G. *J. Phys. Chem. A* **1997**, *101*, 5770.

(6) Platz, J.; Sehested, J.; Nielsen, O. J.; Wallington, T. J. *J. Chem. Soc., Faraday Trans.* **1997**, 93, 2855.

(7) Barnes, I.; Becker, K. H.; Mihalopoulos, N. *J. Atmos. Chem.* **1994**, *18*, 267.

(8) Becker, K. H., Ed. The European photoreactor EUPHORE. Final Report EV5V-CT92-0059; 1996.

(9) Libuda, H. G.; Zabel, F.; Fink, E. H.; Becker, K. H. *J. Phys. Chem.* **1990**, *94*, 5860.

(10) Bierbach, A.; Barnes, I.; Becker, K. H.; Wiesen, E.; *Environ. Sci. Technol.* **1994**, *28*, 715.

(11) Atkinson, R. *J. Phys. Chem. Ref. Data, Monogr.* **1994**, *2*, 1.

(12) Shi, J.; Wallington, T. J.; Kaiser, E. W. *J. Phys. Chem.* **1993**, *97*, 6184.

(13) Taylor, W. D.; Allston, T. D.; Moscato, M. J.; Fazekas, G. B.; Kozlowski, R.; Takacs, G. A. *Int. J. Chem. Kinet.* **1980**, *12*, 231.

(14) Stevens, W.; Van Es, A. *Recueil* **1964**, *83*, 1287.

(15) Thomas, W. Ph.D. Thesis, Bergische University of Wuppertal, Germany, 1998.

(16) Tsalkani, N.; Toupance, G. *Atmos. Environ.* **1988**, *23*, 1849.

(17) Barnes, I.; Donner, B. Tropospheric research programm results 1996−1997. *GSF−Forschungszentrum für Umwelt und Gesundheit GmbH* **1997**, 69.

(18) Wallington, T. J.; Dagaut, P.; Liu, R. Kurylo, M. J. *Int. J. Chem. Kinet.* **1988**, *20*, 177.

(19) Le Calvè, S.; Le Bras, G.; Mellouki, A. *J. Phys. Chem. A* **1997**, *101*, 5489.

(20) Notario, A.; Le Bras, G.; Mellouki, A. *J. Phys. Chem. A* **1998**, *102*, 3112.

(21) Wallington, T. J.; Andino, J. M.; Ball, J. C.; Japar, S. M. *J. Atmos. Chem.* **1990**, *10*, 301.

(22) Olah, G. A.; Vankar, Y. D.; Arvanaghi, M.; Sommer, J. *Angew. Chem.* **1979**, *91*, 649.

(23) Tuazon. E. C.; Aschmann, S. M.; Atkinson, R.; Carter, W. P. L. *J. Phys. Chem. A* **1998**, *102*, 2316.

(24) Bilde, M.; Wallington, T. J.; Ferronato, C.; Orlando, J. J.; Tyndall, G. S.; Estupinan, E.; Haberkorn, S. *J. Phys. Chem.* **1998**, *102*, 1976.

(25) Prinn, R. G.; Weiss, R. F.; Miller, B. R..; Huang, J. Alyea, F. N.; Cunnold, D. M.; Fraser, P. J.; Hartley, D. E., Simmonds, P. J. *Science* **1995**, *269*, 187.